



Journal of Materials Chemistry B

COMMUNICATION

Electronic Supplementary Information (ESI)

Positive Charge Armed Nanoparticles Demonstrate Their Precise Delivery

Performance for Effective Treatment of Chorioretinal Diseases

Wei Wei,^{†a} Dan Zhu,^{†b} Zhenhua Wang,^b Dezhi Ni,^a Hua Yue,^a Shuang Wang,^a Yong Tao^{*cd} and Guanghui Ma^{*a}

^a National Key Laboratory of Biochemical Engineering, Institute of Process Engineering, Chinese Academy of Sciences, Beijing, 100190, PR China. E-mail: ghma@ipe.ac.cn

^b The Affiliated Hospital of Inner Mongolia Medical University, Hohhot, Inner Mongolia, 010050, PR China.

^c Department of Ophthalmology, People's Hospital, Peking University, Beijing, 100044, PR China; Key Laboratory of Vision Loss and Restoration, Ministry of Education, Beijing, 100044, PR China.

^d Department of Ophthalmology, Beijing Chaoyang Hospital, Capital Medical University, Beijing, 100020, PR China. E-mail: drtaoyong@163.com

[†] These authors contributed equally.

Experimental section

Materials and animals: PLGA (Mw =10 kDa, LA : GA = 50 : 50) was purchased from the Institute of Medical Instruments (China). Chitosan (Mw=50000) was ordered from Golden-Shell Biochemica (China), and its derivatives HTCC (N-(2-hydroxy)propyl-3-trimethyl ammoniumchitosan chloride) and CMC (carboxymethyl chitosan) were synthesized according to our previous reports.^{1, 2}. Poly(vinyl alcohol) (PVA) was provided by Kuraray (Japan). Cell-Counting Kit-8 (CCK8) kit was supplied by the Dojindo Laboratories. Dulbecco's Modified Eagle's Medium (DMEM), 4, 6-diamidino-2-phenylindole (DAPI), Cyanine (Cy5), Nile Red, and Alexa Fluor 635 phalloidin were purchased from Molecular Probes. RF/6A cells were supplied by ATCC (American Type Culture Collection). Sprague Dawley (SD) rats were obtained from Vital River Laboratories (Beijing, China). All animal experiments were performed in accordance with the Guide for the Care and Use of Laboratory Animals, and were approved by the Experimental Animal Ethics Committee in Beijing.

Nanoparticle preparation: Uniform-sized PLGA NPs were prepared using the premix membrane emulsification technique as previously reported^{1, 2}. Briefly, the oil phase (3 wt% PLGA dissolved in dichloromethane) and water phase (2 wt% PVA) were mixed by homogenization and poured into the premix membrane emulsification equipment (FMEM-500M). Subsequently, uniform-sized nanodroplets were obtained by extruding the coarse emulsions through the membrane pores. The droplets were stirred and consolidated overnight for evaporation of the organic solvent. To remove the residual PVA emulsifier, the PLGA NPs were washed and collected by centrifugation. For DEX loading, the drug should be dissolved as inner water phase and then encapsulated through W/O/W emulsion.

To prepare neutrally charged NPs (NP⁰), PLGA NPs were mixed with 1 wt% chitosan solution. Chitosan could coat on the surface of the negatively charged CMC NPs based on the electrostatic interaction. After removing the redundant chitosan by centrifugation, the coated chitosan were slightly crosslinked with glutaraldehyde to improve the stability. Similarly, positively charged NPs (NP⁺ and NP⁺⁺) were obtained by coating PLGA NPs with HTCC. The surface charge density could be tunable by controlling the substitution degree of HTCC. These NPs could be further transformed to negatively charged NPs (NP⁻ and NP⁻⁻) by coating with CMC.

Nanoparticle characterization: The average particle size, size polydispersity Index (PDI), and ζ potential of the samples were determined by Zetasizer (Nanoseries, Malvern, U.K.) (n=3). The surface morphology of NPs was observed by scanning electron microscope (SEM, JEOL, Japan). The mobility in the electrical field was tested in 0.25% agarose gel and observed by Bio-imaging systems (MF-ChemiBIS 3.2).

Cytotoxicity test: RF/6A cells were cultured in DMEM with 10% FBS and used to evaluate cytotoxicity of different NPs. Briefly, cells were plated in 96-well tissue culture plates at a cell density of 5×10^4 per well

and incubated at 37 °C under a 5% CO₂ atmosphere. After 24 h, different charged NPs were co-incubated with the RF/6A cells. After 48 h, 20 µl CCK-8 were added to each well and incubated for 2 h. The value was measured using microplate reader (Infinite M200, Tecan) at 450nm wavelength and the cell viability was calculated compared to PBS group (n=3). For high content analysis, the treated cells were fixed with 4% formaldehyde and labeled with nuclear dye DAPI. The cell viability could be analyzed by measuring the integrity and deformation degree of cell nuclear with High Content Screening System (Opera, Perkin Elmer).

Penetration Assay in vitro: RF/6A cells were cultured in DMEM-F12 with 10% FBS. To form a monolayer, these cells were digested, collected, and planted onto transwell membrane. Every two days, the culture medium was replaced, and the trans-epithelial electrical resistance (TEER) was monitored. After one week, the TEER would become stable, indicating the successful establishment of RF/6A cell monolayer. To mimic the intraocular electrical field, each well was set with 100 mV voltage. NPs formulations were then added in the upper chamber. At desired time point, medium containing penetrated NPs was taken from the lower chamber, and the fluorescence intensity sourced from the loaded Nile red was recorded (n=3). The cell monolayer on the membrane could be further used for CLSM imaging (UltraVIEW, Perkin Elmer) after labeling with Alexa Fluor 635 phalloidin.

Ex vivo test: The fresh porcine eyes obtained from a local abattoir were used to access the intraretinal barriers to diffusion. The eyes were opened circumferentially approximately 6 mm behind the limbus and the anterior tissues and the vitreous was separated gently from the neuroretina. The neural retina was soaked in RPMI 1640 solution, separated gently with a glass rod and fixed on the diffusion chamber. After setting with 100 mV voltage, NPs formulations were added in the upper chamber, and the penetrated NPs was taken from the lower chamber. Their fluorescence intensity was recorded to evaluate the penetration performance. The samples could be further used for CLSM observation after treatment with 4% formaldehyde and labeled with DAPI.

Intraocular residence and distribution: Adult SD rats (~200 g) were anesthetized with 2.5% isoflurane and received intravitreal injection (10 µl) of different Cy-5 loaded formulation. At different time points, the rats were executed, and eyes were excised for the investigation of intraocular residence by in vivo imaging system (FXPro, Carestream Health). The excised eyes could be further frozen, sliced, and dyed with DAPI for the observation of NP distribution in retinal sub-layers.

Therapy on choroidal neovascularization model: 7 groups of SD rats were randomly set up and each group contained 5 rats. Each rat was anesthetized by intraperitoneal injection of chloral hydrate and both pupils were dilated with compound glutamine. 6-8 spots were photocoagulated between the retinal vessels in a peripapillary distribution at a distance of approximately 2 disc diameters by using 532 nm diode laser. Laser parameters: spot size 100 µm, power 150-190 mW, and exposure duration 0.2 second. Only a laser lesion with a subretinal bubble indicating that the Bruch's membranes were perforated was

considered effective and thus included in the study. After photocoagulation, the rats were immediately received 5 μ l different formulation (DEX dosage: 200 μ g) via intravitreal injection.

FFA imaging and CNV analysis: After treatment for 14 days, the rats were anesthetized and intraperitoneal injected with 20% fluorescein sodium. FFA image was captured using retinal imaging microscope (Phoenix Micron IV, Phoenix Research Labs). To make CNV visualized and quantified, the rats were anesthetized and injected with FITC-dextran (50 mg dissolved in 10ml PBS) via the left ventricle. When the skin of mouth, nose, arms and legs turn yellow, success perfusion was confirmed. The rats were executed, and eyes were excised. Neovascularization was observed under CLSM after flat-mount choroid was prepared. The captured images were analyzed, and CNV area was measured by software Image Pro Plus 6.

Intraocular pressure measurement: IOP of awake rats was measured with a handheld electronic tonometer (TonoPen AVIA, Reichert). Tonopen was applied perpendicularly to the apical side of the cornea. The data of IOP showed on Tonopen was the mean of ten times consecutively and automatically measurement results. The final data was a mean of IOP results after three times use of Tonopen. In order to avoid circadian IOP changes, all measurements were taken at the same hour of the day.

Statistical analysis: Statistical analysis of data was performed by Student's t-test for multiple groups. All results were expressed as mean \pm standard (s.d.) error. Asterisks denote significant differences (* $p < 0.05$; ** $p < 0.01$).

References

- 1 P.-P. Lv, W. Wei, H. Yue, T.-Y. Yang, L.-Y. Wang and G.-H. Ma, *Biomacromolecules*, 2011, **12**, 4230-4239.
- 2 W. Wei, P.-P. Lv, X.-M. Chen, Z.-G. Yue, Q. Fu, S.-Y. Liu, H. Yue and G.-H. Ma, *Biomaterials*, 2013, **34**, 3912-3923.

Formulation	Zeta (mv)	Size (nm)
NP--	-32.6	142.0
NP-	-16.6	143.5
NP0	-1.2	138.4
NP+	+16.5	139.2
NP++	+36.4	140.8

Table S1. Characterizations of zeta potential and particle size of different NPs, demonstrating the success of surface decoration on PLGA NPs with different charge and density.

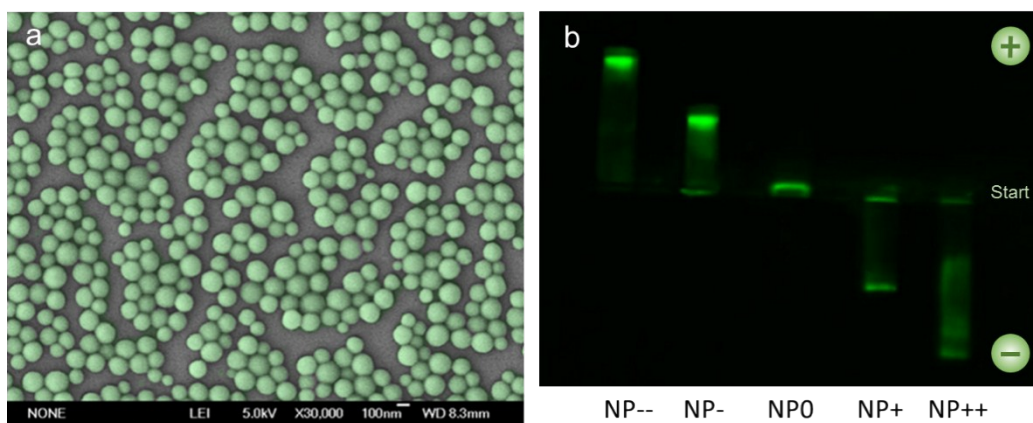


Fig. S1. Scanning electron microscope (SEM) image of PLGA NPs (a) and the mobility in agarose gel (b) after decoration with different charge.

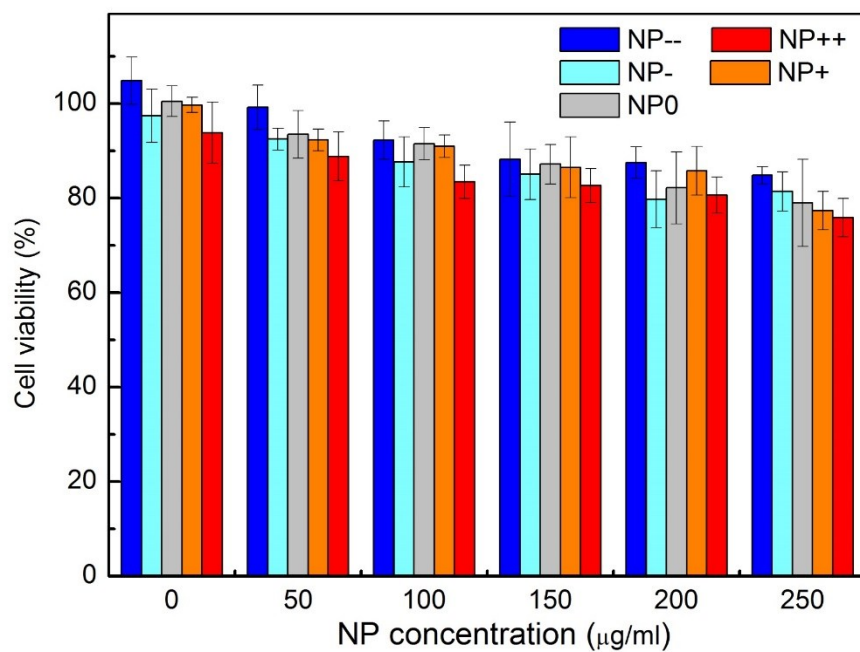


Fig. S2. Cytotoxicity evaluation of different NPs by CCK-8 analysis. Very slightly decreased viabilities (<20%) were observed when RF/6A cells were treated with 250 µg NPs, suggesting their good biocompatibility.

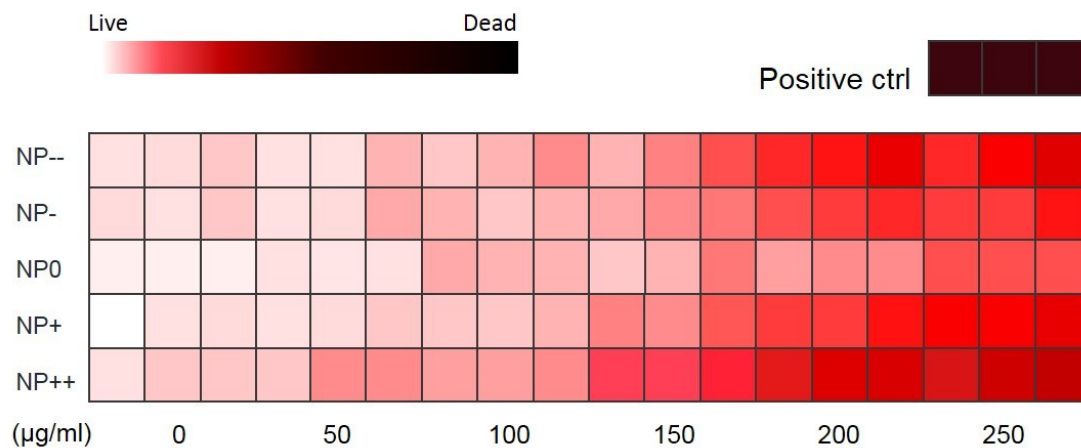


Fig. S3. Cytotoxicity analysis of different NPs by High Content Screening. The data again demonstrated the good biocompatibility of NPs on RF/6A cells.

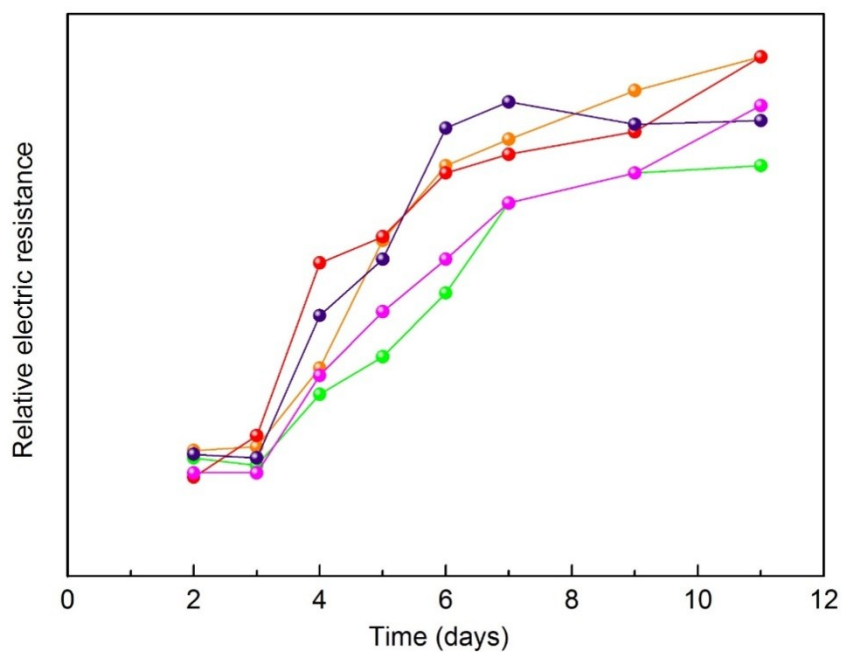


Fig. S4. TEER of RF/6A cells during culture on Transwell membrane. The value became stable after one week, suggesting the formation of RF/6A cell monolayer. The TEER values in each well were indicated by different colors.

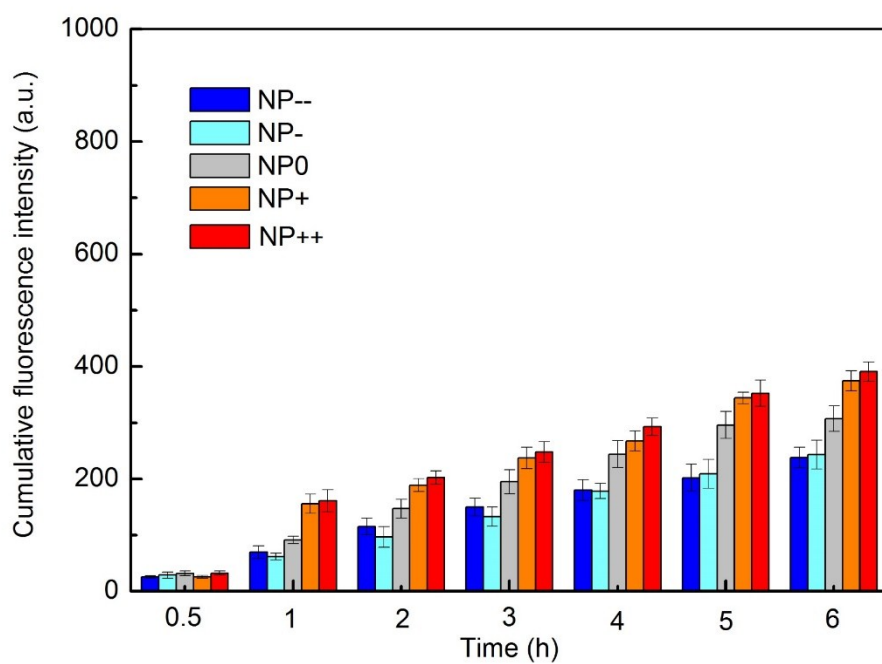


Fig. S5. Permeation of different NPs across the EF/6A cell monolayers.

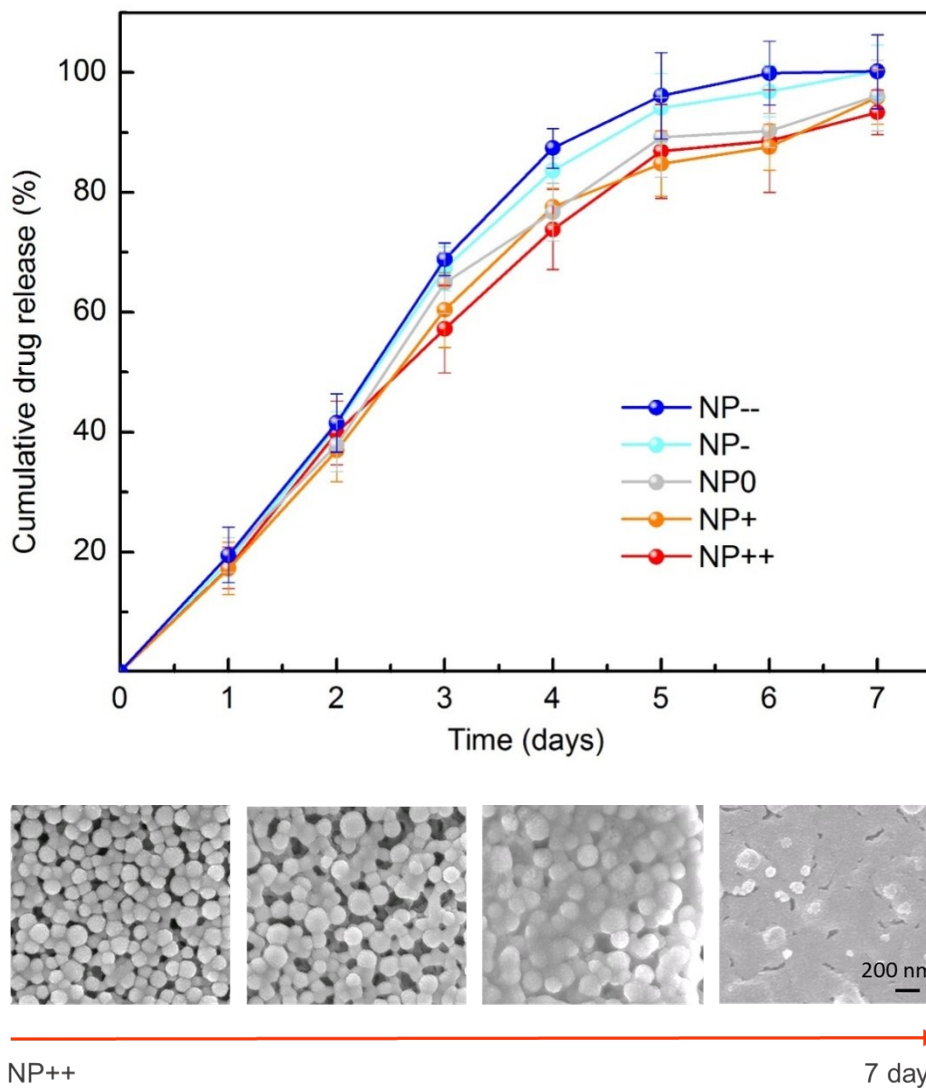


Fig. S6. In vitro drug release profiles and comprehensive NP degradation process. More than 90% DEX could be released from the well-degraded NPs during one week. Compared with negatively charged NPs, the positively charged NPs exhibited a bit slower release profiles due to the electrostatical interaction between DEX (sodium phosphate) and NPs.